Blucher Material Science Proceedings
Novembro de 2014, Número 1, Volume 1
www.proceedings.blucher.com.br/evento/mm-fgm2014

B_4C and Fe-B Addition Influence on the Cavitation Resistance of the Plasma PTA Fe-Mn-Si Coating

Luciana Leite Silveira[1], Anderson Geraldo Marenda Pukasiewicz[2]

[1]*UTFPR Federal University of Technology - Paraná, luciana.llsilveira@gmail.com*
[2] *UTFPR Federal University of Technology - Paraná, anderson@utfpr.edu.br*

Abstract

The aim of this work is study the effect of the FeB and B4C addition on the microstructure and cavitation resistance of the plasma PTA Fe-Mn-Si coating. The hardness of the iron-based alloy can be increased by adding a certain amount of carbides, such as B4C and Fe-B, leading to formation of secondary phases of high hardness. Three alloys Fe-Mn-Si with B4C and FeB additions were deposited by plasma transferred arc process in AISI 304 plates. The microstructure and dilution were analyzed by optical microscope and scanning electronic microscope. Mechanical properties were analyzed by microhardness and cavitation resistance was analyzed by ultrasonic ASTM G32 indirect method. It was found thus far that the addition of boron either by adding Fe-B, such as by adding B4C caused an increase in the wettability of the alloy and consequently better deposition. We also observed a significant change in microstructure, forming higher levels of secondary phases and the formation of a hipoeutetic structure. There was also an increase of the hardness of coatings deposited with addition of boron. It was observed an increase on the cavitation resistance of the coating with FeB and B4C addition

Keywords: cavitation, boron, plasma transferred arc

1. Introduction

The cavitation erosion is a process where there is the formation and collapse of vapor bubbles in a fluid, formed due to the localized pressure reduction, conducted thereafter to a region of higher pressure than the steam and then condensates. This collapse of vapor bubbles produces extremely high pressures that often damage the surface of the material, causing it to erode. [1]

Hydropowerplants' turbines, valves, pumps and ships' propellants and other hydraulic components show significant maintenance and repair costs increase by cavitation damages, generating loss of time, and equipment life reduction, even reducing the efficiency of the equipment [2, 3]

The hardness of the iron-based alloy can be increased by adding a certain amount of high hardness carbides, such as boron carbides. The addition of boron leads the coating to present the formation of a eutectic with 3.8%, creating Fe_2B as the secondary phase, increasing the resistance of the alloy, and reducing the melting point, allowing a better deposition condition. [4]

The plasma transferred arc process, PTA, uses the arc in special operating conditions, which acts as an extremely stable heat source, which allows the welding of most metals. One of the main advantages of the PTA process is the use of powder as a metal addition. The use of the powder increase the flexibility of the process [5].

The aim of this work is study the effect of the secondary phase formation on the cavitation resistance of the plasma PTA Fe-Mn-Si coating. Secondary phase were formed by FeB and B4C addition on the Fe-Mn-Si coating.

2. Methods

A Fe-Mn-Si alloy with similar levels of Boron by adding B_4C and Fe-B powders, was selected for analysis. The powders were deposited by the plasma PTA process on AISI 304 austenitic stainless steel plates, of composition 0.08% C, 2% Mn, 0.75% Si, 0.045% P, 0.03% S, 19% Cr, 9% Ni and 0.10% N. The deposition parameters used were 120 A of current, powder feed rate of 8 kg/h and deposition velocity of 10 cm/min. The composition of the deposited alloy can be seen in Table 1.

Anderson Gerald Marenda Pukasiewicz, UTFPR Av. Monteiro Lobato km04, s/n, Ponta Grossa-PR CEP 84016-210

Table 1. Chemical composition of the Fe-Mn-Si alloys with different additions of Fe-B and B4C.

Liga	Chemical composition				
	Fe	C	Mn	Si	B
Fe-Mn-Si	79,25	0,41	17,20	3,14	--
Fe-Mn-Si + Fe-B	78,17	0,40	16,91	3,48	1,04
Fe-Mn-Si + B_4C	78,16	0,4	16,91	3,49	1,04

The samples were metallographic prepared in an automated system. The grinding was realized with a 350 rpm rotation, 20N of force, using sandpaper of 220, 320, 400, 600 and 1200 mesh. For polishing, at 150 rpm and 15N of force, were used 9, 3 and 0.25 μm diamond suspensions and 0.04 μm colloidal silica. After this procedure, the samples were chemical etching for revelation of the microstructure. The chemical treatments used were Villela's, and the other chemical etching was had the composition of 10 mL H_2O, 1.2% $K_2S_2O_5$ and 0.8% of NH_4F_2 [6].

The samples were analyzed by optical microscopy for evaluation of the formed microstructure, formation of secondary phases and presence of defects. The phases present in the coatings were identified by X-ray Diffraction (XRD). The analysis of the mechanical properties was performed by Vickers hardness technique using a 300 gf load.

Subsequently the samples were prepared for cavitation testing. The samples were cutted to form a flat surface, and afterwards grinded and polished. The specimens were tested in cavitation ultrasonic testing equipment, following ASTM G32 standart. The indirect method with distance of 500mm between the sonotrode and sample, and frequency of 80 kHz ± 0.5 was used. It was deionized water with temperature controlled at 20 ° C ± 1 ° C. The testing intervals were initially 20 min and then posteriorly 40 min until complete 240 min of cavitation test. After each interval, mass loss measurements were performed, and then the samples were analyzed by Optical and Eletronical Microscope for evaluation of microstructural change of the coatings.

3. Results

Initially, the phase of the deposited coatings was characterized by X-ray diffraction. The spectrum of the Fe-Mn-Si alloy showed the formation of austenite γ and martensite ε and α', and the Fe-Mn-Si alloys with additions of Fe-B and B_4C showed the formation of austenite γ as primary phase and FeB and Fe_2B as secondary phases. It was noticed that Boron adition prevent martensite formation on the alloy.

The microstructure of the coatings were analyzed by optical microscopy and scanning electron microscopy – SEM. Figure 1 (a) shows the microstructure of the Fe-Mn-Si alloy coating observed in optical microscope, in which it is possible to observe the dendritic microstructure composed of austenite γ and martensite ε and α '. The martensite formation on this alloy can be occurred by the rapid cooling observed on the PTA process deposition and can also occurred by surface deformation during grinding and polishing of metallographic sample preparation.

Figure 1 (b) shows the microstructure of the Fe-Mn-Si alloy with Fe-B addition, in which it can be seen that the coating consists of a dendritic and an interdendritic area. The eutectic consists of austenite γ as primary phase and Fe_2B and/or FeB as secondary phase. The same configuration was observed in the Fe-Mn-Si alloy with B_4C addition, shown in Figure 1 (c).

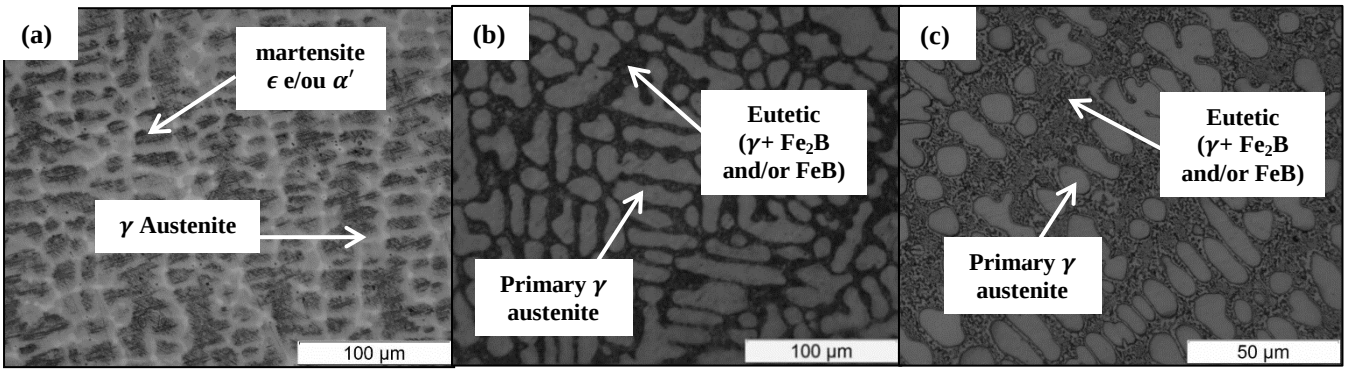

Figure 1: Dendritic microstructure of (a) phases austenite γ and martensite ϵ and α', Fe-Mn-Si alloy, optical microscope, 500x, primary γ austenite and eutectic phase consisting of γ austenite and Fe_2B and/or FeB, (b) Fe-Mn-Si alloy with addition of Fe-B, optical microscope, 500x, (c) Fe-Mn-Si alloy with addition of B_4C, optical microscope, 1000x.

Microstructure of the coatings were also analyzed by SEM microscope, where the martensite formation and the eutectic formation were better evaluated. The martensite observation on this kind of alloy is well described by [6]. On the Fe-Mn-Si alloy with B_4C it was observed the eutectic microstructure occurred by the Boron addition, and the alloy with FeB addition showed a very similar behavior.

One important aspect observed is the porosity reduction with the FeB and B_4C addition. The addition of boron in the Fe-Mn-Si alloy promoted a better wettability of the coating, due to the formation of a eutectic, causing a decrease in the alloy's

melting point. Probably this aspect improve the quality of the coating reducing the porosity of the alloy. The formation of the phase Fe-B was observed by XIBAO [7] and in AMUSHAHI et. al [4].

Vickers microhardness analysis results of the samples with addition of Fe-B and B4C presented an increase in the average hardness, which can be observed in Table 2.

Table 2. Average Vickers Hardness of the samples of the Fe-Mn-Si alloys.

Alloy	Average Vickers Hardness (HV)
Fe-Mn-Si	259,90
Fe-Mn-Si + Fe-B	424,80
Fe-Mn-Si + B_4C	548,79

The Fe-Mn-Si alloy with additions of Fe-B and B4C has also presented an increase in the average hardness of the samples, and the higher values presented by the B_4C alloy can be attributed to the higher concentration of Fe-B phase observed in DRX. Despite the hardness increase, the values were inferior than those observed by [4, 7], due to the lower addition of boron used in this study.

The mass loss due to the cavitation testing of the alloys was measured at different intervals from 0 to 240 min. The samples with additions of Fe-B and B4C suffered a lower mass loss rate, compared with the base Fe-Mn-Si alloy, Table 3. Fe-Mn-Si alloy showed a higher mass loss at the beginning of the testing. The initial higher mass loss of the Fe-Mn-Si base alloy, on the first measurement after 20 minutes, probably occurred mainly because of the higher porosity of the samples.

Table 3: Cumulative mass loss of the samples of the Fe-Mn-Si alloys after 240min.

Alloy	Cumulative mass loss after 240 min (mg)
Fe-Mn-Si	155,2
Fe-Mn-Si + Fe-B	27,8
Fe-Mn-Si + B_4C	30,1

The porosity can act as a nucleus for the beginning of the cavitation process, Figure 2 (a). After this short period of time, the mass loss occurred on the entire surface, as observed in Figure 2 (b). The deformation in the Fe-Mn-Si alloy during the test occurs because of the energy absorption of the implosion of the bubbles, which forms martensite ε during deformation of the austenite γ [8].

These deformation structures were not so clearly observed in alloys with FeB and B_4C addition after 40min of cavitation tests. Probably the microstructure refining and the increase of the hardness affect the $\gamma \rightarrow \varepsilon$ transformation mechanism retarding the transformation.

The Fe-Mn-Si alloys with FeB and B_4C addition showed lower mass loss at the beginning of the process, where the mass loss was concentrated at the eutectic regions. It was observed a difference in the mass loss wear distribution in the alloys, with a more homogeneous distribution in the alloy without addition of boron, and a more localized wear distribution in the alloys with boron addition. The difference in mass loss wear distribution in materials with presence of carbides was observed by CUPPARI [9], which studied the levels of stress suffered by the matrix and the second phase of the material.

Adding boron to the alloy was effective to reduce the cavitation mass loss, and the differences between the stress suffered by the primary and the eutectic phase led to a more located wear in the eutectic area, that contained the boron carbides.

4. Conclusions

The addition of boron to the Fe-Mn-Si alloy, by the compounds FeB and B_4C, was efficient to increase the hardness of the coatings of alloys due to the formation of a microstructure containing the secondary phases FeB and Fe_2B of high hardness.

It was also achieved a decrease in mass loss by adding boron to the Fe-Mn-Si alloy, and a difference in the distribution of the mass loss wear of the coating was observed on the samples with boron addition. The Fe-Mn-Si alloy showed a more homogeneous mass loss. In the alloys with boron addition, due to the eutectic phase formation, the mass loss occurred mainly in these regions.

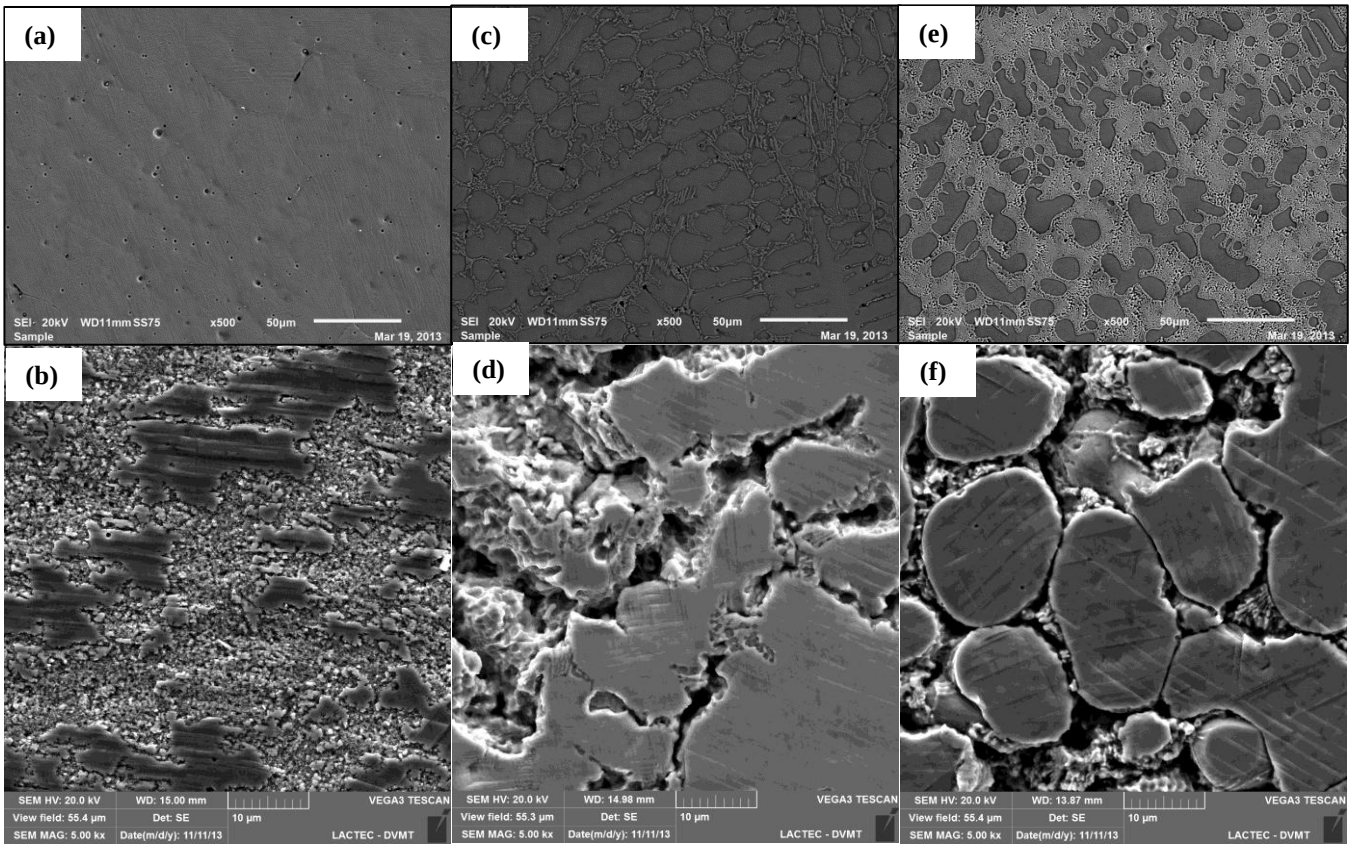

Figure 2: Evolution of wear over time due to cavitation testing: Fe-Mn-Si alloy at (a) 0 min of test, (b) 120 min, Fe-Mn-Si alloy with addition of Fe-B at (c) 0 min, (d) 120 min, Fe-Mn-Si alloy with addition of B_4C at (e) 0 min, (f) 120 min.

Acknowledgements

To the Universidade Tecnológica Federal do Paraná, Ponta Grossa Campus and LACTEC, for the availability of research structure and Araucaria Foundation for Scientific Initiation scholarship.

References

1. L.L., Sheir, et.al, Corrosion: Metal/Environment Reactions vol01, 3ª edição. Butterworth Heinemann. Oxford. (1994).
2. P. March, J. Hubble, Jerry: Evaluation of Relative Cavitation Erosion Rates For Base Materials, Weld Overlays, and Coatings. Report No. WR28-1-900-282, Tennessee Valley Authority Engineering Laboratory, Norris, TN., 1996
3. Huth, Hans-Jörg, Fatigue design of hydraulic turbine runners, Trodheim, Norway 2005, 178 f., Engineering Doctor Thesis, Department of Engineering Design and Materials, Norwegian University of Science and Technology.
4. AMUSHAHI, M.H.; ASHFRAFIZADEH, F.; SHAMANIAN, M. Characterization of boride-rich Hardfacing on Carbon Steel by Arc Spray and GMAW Processes, Surface and Coatings Technology, 2004, p. 2723-2728, 2010.
5. MARQUES, Paulo Villani; MODENESI, Paulo José. Soldagem I: Introdução aos Processos de Soldagem. Departamento de Engenharia Mecânica, Universidade Federal de Minas Gerais, Belo Horizonte, 2006.
6. NASCIMENTO, Fabiana C.; SORRILA, Flávio V.; OTUBO, Jorge; MEI, Paulo R. Stainless Shape Memory Alloys Microstructure Analysis by Optical Microscopy using differents Etchants, Acta Microscopica, 2003,1-5.
7. XIBAO, Wang. The composite Fe-Ti-B-C coatings by PTA powder surfacing process. Surf. Coat. Technol. 192(2-3) (2005) 257-262.
8. Xiaojun, Z., Procopiak, L.A.J., Souza, N.C., d'Oliveira, A.S.C.M., Phase transformation during cavitation erosion of a Co stainless steel, Materials Science and engineering A, v. 358, nº 1-2, p. 199-204, out. 2003
9. CUPPARI, M. G. Di V.; SOUZA, R.M.; SINATORA, A. Effect of hard second phase on cavitation erosion of Fe–Cr–Ni–C alloys. Second International Conference on Erosive and Abrasive Wear, Elsevier: 2004